Forest Chemicals Revew
www.forestchemicalsreview.com
ISSN: 1520-0191
July-August 2021 Page No. 974-988
Article History: Received: 12 May 2021 Revised: 25 June 2021 Accepted: 22 July 2021 Publication: 31 August 2021

Experimental Study on Slag Discharge of Sandstone in Small-Angle Reverse Drilling and Reaming

Dongyang Geng[1,2], Yongqiang Shi[3], Xiufeng Liang[1,2], Jianguang Niu[1,2*], Chunyan Gao[1,2]

[1]College of Urban Geology and Engineering, Hebei GEO University, Shijiazhuang, HeBei, China
[2]Hebei Technology Innovation Center for Intelligent Development and Control of Underground Built Environment, HeBei, China
[3]Liaoning Municipal Engineering Design and Research Institute Co., Ltd. Liaoning, China
*Corresponding Author.

Abstract:

When oil and gas pipelines cross mountains, reverse drilling is adopted, and rock slag formed by drilling falls by its weight. Under the construction condition of small-angle reverse well drilling, the rock slag cannot fall by its weight when the drill bit reams. Based on the analysis of small-angle reverse well drilling for oil and gas pipeline crossing the mountain, a slag discharge test device is designed, and the slag discharge effect is tested from four angles of 20°, 25°, 30°, and 35°. Combined with the actual construction conditions, 2.5m^3/h, 5m^3/h, and 10m^3/h water flow is used to assist slag removal, to approximately simulate the process of rock slag falling from the broken rock surface during drilling with small-angle reverse drilling. At the same time, the velocity of rock slag was monitored during the experiment, and the kinematic characteristics and mechanism of rock slag falling were analyzed. The research shows that when the stability coefficient k of sandstone slag is less than 0.7, the slag can be fully discharged, and the starting speed can be calculated by using the improved formula of Stirling. Under the condition of 20-35°, the critical start-up speed of slag-carrying water flow under different displacement is in the range of 0-5m/s; When the drilling angle of the reverse well is 20° or above, the sandstone slag has an obvious slag removal effect with the aid of water flow of 10 m^3/h. When the whole angle of the reverse well is 30° or above, the sandstone slag has an obvious slag removal effect with the aid of 5m^3/h water flow. The research of small-angle anti-drilling in oil and gas pipeline crossing mountains is an innovation in the construction technology of oil and gas pipeline crossing mountains, which is not only conducive to promoting the progress of oil and gas pipeline construction technology. It can also provide a reference for the research of construction technology in other areas of oil and gas pipelines and has important research significance.

Keywords*: Raise drilling; oil and gas pipeline; trenchless technology; slag discharge.*

Forest Chemicals Revew
www.forestchemicalsreview.com
ISSN: 1520-0191
July-August 2021 Page No. 974-988
Article History: Received: 12 May 2021 Revised: 25 June 2021 Accepted: 22 July 2021 Publication: 31 August 2021

I. INTRODUCTION

During the reaming construction of oil and gas pipelines, the broken rock slag falls into the lower roadway due to its weight, and then the rock slag is removed by rock loader and belt conveyor. There is no repeated crushing phenomenon and the drilling effect is high; Fast drilling speed; Good construction conditions. In oil and gas pipeline engineering, some areas have strict requirements on-ground environmental protection, and it is forbidden to damage ground vegetation, so it is impossible to carry out ground excavation in oil and gas pipeline construction. [1] To meet the requirements of small-angle construction of pipeline engineering, it is necessary to adopt the construction method of small-angle reverse well drilling. In the process of small-angle reverse drilling, the broken rock slag cannot be discharged downward by its weight, which brings difficulties to the construction, so it is necessary to consider forcing it to be discharged downward by various means. In this paper, the problem of slag discharge after small-angle reverse drilling and reaming is studied experimentally.

II SPECIMEN PREPARATION AND TEST EQUIPMENT

2.1 Test instruments

High-frequency vibrating screen, sand screen, LS300A flow velocimeter, water pump and other instruments are used in the test (see Fig 1). See table I for related models and parameters.

High frequency vibrating screen instrument Flow velocimeter Electronic induction scale

Fig 1: Experimental instrument

TABLE I. Model and parameters of experimental instruments.

device name	model	parameter
High frequency vibrating screen	GZS-1 type	Frequency: 500 times/min; Voltage: 220V

Forest Chemicals Revew
www.forestchemicalsreview.com
ISSN: 1520-0191
July-August 2021 Page No. 974-988
Article History: Received: 12 May 2021 Revised: 25 June 2021 Accepted: 22 July 2021 Publication: 31 August 2021

instrument		
Sand screen cloth	national standard	Stone sieve size: 2. 36mm-70mm.
Electronic induction scale	Type HF-2kN	The measuring range is 0 ~ 2kn.
Flow velocimeter	Type LS300A	0-25mm in size.
water pump	50LZ2H	Power 37; Voltage: 220V

2.2 Layout of test bench.

(1) Semi-circular cross-section concrete pipe was used to simulate the slag discharge hole in the experiment. To fit the actual slag discharge environment, the inner wall of the concrete pipe was evenly scratched horizontally (see Fig 2).

Fig 2: Formwork and inner wall scratch of concrete pipe.

(2)The rock slag collecting plate is arranged at the bottom of the semi-circular cross-section slag discharge hole to collect rock slag.

(3)The angle adjusting device is arranged at the end of the semi-circular cross-section slag hole to adjust the slope of the slag hole.

(4)The rock slag baffle is designed at the initial end of the semi-circular cross-section slag chute. In the test preparation stage, the rock slag baffle is filled with rock slag.

(5)The water pipe and water baffle are designed at the initial end of the semi-circular section slag hole. By controlling the amount of water sprayed from the water pipe, the lubrication conditions with different degrees of water are simulated. Fig. 3 is the layout of the slag discharge test.

Forest Chemicals Revew
www.forestchemicalsreview.com
ISSN: 1520-0191
July-August 2021 Page No. 974-988
Article History: Received: 12 May 2021 Revised: 25 June 2021 Accepted: 22 July 2021 Publication: 31 August 2021

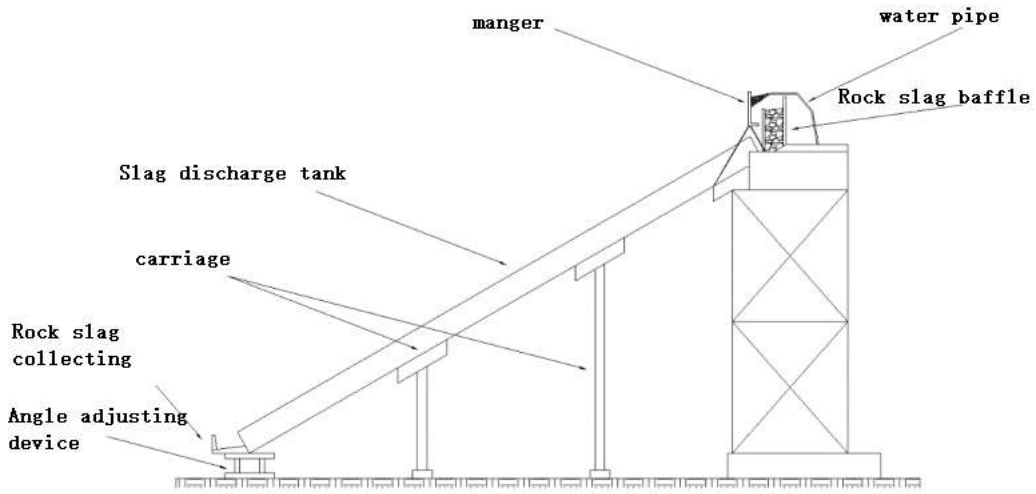

Fig 3: Layout of rock slag slip test.

2.3 experimental steps.

Step 1, put the sandstone slag used in practical engineering into a high-frequency vibrating screen for particle size screening.

Step 2, Grouping sandstone rock slag in natural accumulation state, each of which is 0. 08m^3 (i. e. the amount of rock slag produced by drilling lm with drill bit); Put the fallen rock slag on the top of the chute of the test bench, and use a partition to prevent it from falling. See fig. 4 for the slag removal process.

Fig 4: Slag discharge process diagram

Step 3, open the water valve, so that the water flows from the upper part of the rock slag and falls on the baffle to ensure that the initial velocity is 0; Spray water for 5min to make the water flow fully wet the surface of the slag discharge tank. In this experiment, four angles, 20, 25, 30, and 35, were selected to analyze the slag removal effect. Combined with actual working

Forest Chemicals Revew
www.forestchemicalsreview.com
ISSN: 1520-0191
July-August 2021 Page No. 974-988
Article History: Received: 12 May 2021 Revised: 25 June 2021 Accepted: 22 July 2021 Publication: 31 August 2021

conditions, water flows of 0, 5, and 10 m^3/h are used to drain water from the upper part and assist in slag discharge.

Step 4 open the clapboard to make the rock slag fall, and measure the speed by the flow velocimeter installed in each section of the slag discharge tank; Continue to drain water for 2 min until all parts of rock slag are completely stationary. The LS300A flow velocimeter is used in the test, with an interval of 1m, which is set in each section of the slag discharge tank. The rock slag collecting plate is designed at the bottom of the semi-circular cross-section slag discharge hole, and the rock slag is collected after being fully drained.

Step 5 close the water valve, divide the chute into sections every 5m, collect and dry the discharged sandstone slag, and then weigh them separately.

Step 6 Change the angle of the slag discharge tank and the water flow, and repeat the above steps. The slag chute is evenly divided into four sections. From the initial end, the residual rock slag in each channel is collected and weighed in turn, which is marked as W_1, W_2, W_3, and W_4. Rock slag on the ground is marked as W5. See Fig 5 for the site of the slag removal test bench.

Fig 5: Site map of the slag discharge test bench

III THEORETICAL ANALYSYS

3.1 Mechanical equilibrium analysis of unsaturated soil

Sandstone slag is in unsaturated state before adding water. According to the shear strength formula of unsaturated soil:[2]

$$\tau = C' + (\sigma_f - \mu_a)_f \tan\varphi' + (\mu_a - \mu_\omega)_f \tan\varphi^b \qquad (1)$$

Where, $C'$is the intercept of Mohr-Coulomb shear stress axis and the extension of failure envelope, the net normal stress and matrix suction at the shear stress axis are both 0, and is also called effective cohesive force (effective cohesive force is very small due to the unconsolidated solid loose material); is the total normal stress on the failure surface during failure; is the pore

Forest Chemicals Revew
www.forestchemicalsreview.com
ISSN: 1520-0191
July-August 2021 Page No. 974-988
Article History: Received: 12 May 2021 Revised: 25 June 2021 Accepted: 22 July 2021 Publication: 31 August 2021

air pressure on the failure surface during failure; is the pore water pressure on the failure surface during failure, and the failure surface gradually rises with the increase of water volume in the test. [3-8]

$(\sigma_f - \mu_a)_f$ is the net normal stress state on the failure surface during failure; is the matrix suction on the failure surface during failure, and φ′ is the internal friction angle related to the state variable of net normal stress $(\sigma_f - \mu_a)_f$; φ^b is the rate at which shear strength increases with matrix suction $(\sigma_f - \mu_a)_f$; is the shear strength caused by matrix suction. [9-10]

At the beginning of the test, the baffle and water flow were opened, and the sandstone slag was in a solid unsaturated loose state, and then the water content of the slag gradually increased and reached a saturated state. The matrix suction caused the shear strength to disappear, the water pressure increased, and the effective stress decreased. At this stage, the rock slag did not fall with the water flow, but the rock slag pile was deformed and displaced. The relationship between shear strength of rock slag pile and pore water pressure is as follows:

$$\tau = C + (\sigma - \mu_\omega)\tan\varphi \tag{2}$$

Where is the cohesive force of the rock slag pile; is the internal friction angle of the rock slag pile in saturation state. Divide the slag chute into four sections evenly, and collect and weigh the residual rock slag in each section from the initial end, which is marked as W1, W2, W3, and W4. Collect the rock slag in the bottom rock slag collection plate, weigh it and mark it as W5. Considering that part of silty rock slag will be washed away with water flow under the condition of adding water, the calculation method of rock slag rate without adding water is as follows:[11]

$$\frac{W_5}{W_{total}} \times 100\% \tag{3}$$

Under the condition of adding water, the calculation method is:

$$\eta = 1 - \frac{W_1+W_2+W_3+W_4}{W_{total}} \times 100\% \tag{4}$$

3.2 Analysis of starting velocity of rock slag water flow.

Sandstone slag will be mixed with water flow in the process of slag removal by adding water, so the process of slag removal by sandstone can be compared with debris flow. At present, the calculation of debris flow velocity is mainly based on empirical and semi-empirical formulas, which can be generally divided into three types: sparse debris flow velocity calculation formula, viscous debris flow calculation formula, and large rock movement velocity calculation formula in debris flow. According to the above calculation of bulk density, it can be seen that the bulk density values are all below 1. 8g/cm^3, so the debris

Forest Chemicals Revew
www.forestchemicalsreview.com
ISSN: 1520-0191
July-August 2021 Page No. 974-988
Article History: Received: 12 May 2021 Revised: 25 June 2021 Accepted: 22 July 2021 Publication: 31 August 2021

flow in the Zili River gully is sparse, and the flow velocity is calculated according to the calculation formula of sparse debris flow.

(1) Adopt the comprehensive formula recommended by Southwest Research Institute of Railway Research Institute. [12]

$$V_c = \frac{M_c}{\sqrt{\gamma_H \varphi + 1}} \cdot R_c^{2/3} I^{1/2} \quad (5)$$

In which, v is the velocity of debris flow and v is the hydraulic slope of debris flow, which can generally be replaced by the longitudinal slope of gully bed. The formation area, circulation area, and accumulation area are taken as 85‰, 130‰、 268‰ respectively. R is the resistance coefficient outside the gully bed, with a value of 12. 9. as the severity of solid matter in debris flow and a value of 2. 6g/cm^3. as the hydraulic radius, which can be generally replaced by the average water depth. is the sediment correction coefficient:[13]

$$\varphi = \frac{\gamma_c - 1}{\gamma_H - \gamma_c} \quad (6)$$

(2) The formula recommended by the Scientific Research Institute of the Second Railway Survey and Design Institute is improved from the data of Laogangou and Fawogou in the Dongchuan area and Yinong River in the Xichang area. [14]

$$V_c = \frac{M_c}{\sqrt{\gamma_H \varphi + 1}} \cdot R_c^{2/3} I^{1/6} \quad (7)$$

Type, for the ditch bed resistance coefficient, can be determined by Ding Yushou resistance coefficient table, take 10. 2; Other symbols are the same as above.

(3) Recommended formula of Beijing Municipal Design Institute

$$V_c = \frac{m}{\sqrt{\gamma_H \varphi + 1}} \cdot R_c^{2/3} I^{1/10} \quad (8)$$

Where m is the external resistance coefficient of the trench bed, which can be found from Liu Dezhao's external resistance coefficient table (see Table Ⅱ), and taken as 7. 5; Other symbols are the same as above. R the hydraulic radius of debris flow is sometimes replaced by the average water depth (h). [15]

Comparing the chute with the river channel bed, it can be known that the river reach is straight, the riverbed is flat, the cross-section is rectangular or parabolic boulders or loess riverbed, and when the average grain size is 0. 001-0. 08m, the longitudinal gradient of the chute is I>0. 015m, the m value can be taken as 7. 5.

Forest Chemicals Revew
www.forestchemicalsreview.com
ISSN: 1520-0191
July-August 2021 Page No. 974-988
Article History: Received: 12 May 2021 Revised: 25 June 2021 Accepted: 22 July 2021 Publication: 31 August 2021

TABLE II. External resistance coefficient of Liu Dezhao.

CATEGORY	CHARACTERISTICS OF RIBER CHANNEL AND SECTION	M
I	The trench is straight and flat, with an average grain size of 0. 005-0. 050m, and the cross section is rectangular and parabolic.	9. 4
II	The trench is straight and level with an average grain size of 0. 02-0. 10m; Or a class I riverbed which is domed and uneven.	7. 5
III	The trench is relatively straight with an average grain size of 0. 04-0. 30m; Or more curved.	5. 8
IV	The trench is relatively straight with an average grain size of 0. 2-0. 6m; Or a class III riverbed which is curved and messy.	4. 6
V	In II, III and IV ditch sections, the bend is large, the cross section of the ditch bed is not very regular, and large boulder or tree vegetation blocks the riverbed.	3. 4

IV ANALYSIS OF TEST RESULTS

4.1 Analysis of experimental results of slag discharge effect.

See table III for the measured data of slag removal effect. According to the data in the table, arrange the data into a histogram as shown in Fig 6.

TABLE III. Sandstone slag discharge effect table (unit: kg)

WATER DISCHARGE 0/m^3						WATER DISCHARGE 2. 5/m^3				
ANGLE	W_1	W_2	W_3	W_4	W_5	W_1	W_2	W_3	W_4	W_5
20°	102	0	0	0	0. 08	5. 5	75. 8	7. 2	8. 8	9. 3
25°	100. 85	0. 8	0. 1	0. 1	0. 15	3. 5	2. 2	3. 7	71. 7	20. 01
30°	15. 6	71. 9	13. 4	0. 25	0. 6	1. 4	1. 7	1. 2	77. 1	21. 85
35°	1	1. 5	10. 7	87. 5	3. 25	0. 3	0. 5	0. 2	51. 3	49. 9
WATER DISCHARGE 5/m^3						WATER DISCHARGE 10/m^3				

Forest Chemicals Revew
www.forestchemicalsreview.com
ISSN: 1520-0191
July-August 2021 Page No. 974-988
Article History: Received: 12 May 2021 Revised: 25 June 2021 Accepted: 22 July 2021 Publication: 31 August 2021

ANGLE	W_1	W_2	W_3	W_4	W_5	W_1	W_2	W_3	W_4	W_5
20°	5. 2	4. 3	4. 5	78. 5	14. 1	1. 5	1. 6	3. 7	2. 8	95
25°	1. 7	0. 95	0. 5	58. 1	40. 7	0. 3	0. 2	0. 35	1. 5	99. 15
30°	0. 3	0. 1	0. 25	1. 15	98. 2	0	0	0	1. 6	93. 46
35°	0	0	0	25. 7	76. 5	0	0	0. 36	0. 85	97. 95

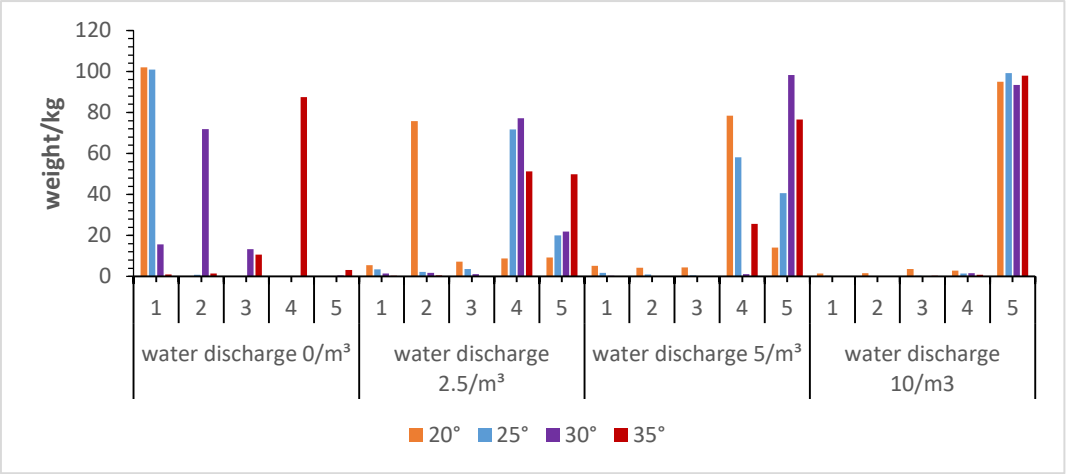

Fig 6: Sand slag discharge effect diagram

According to the data, when the reaming angle of reverse well drilling is 20, the slag discharge of sandstone is sufficient under the auxiliary condition of water flow and drainage of $10m^3/h$, and the slag discharge under this condition is feasible. When the reaming angle of reverse well drilling is 25, slag removal is still sufficient with the aid of water flow of $10m^3/h$, and slag removal is feasible under this condition. When the reaming angle of reverse well drilling is 30, slag removal is sufficient under the auxiliary conditions of $5m^3/h$ and $10m^3/h$, and slag removal is feasible under this condition. When the reaming angle of reverse well drilling is 35, slag removal is sufficient under the auxiliary conditions of $5m^3/h$ and $10m^3/h$, and slag removal is feasible under this condition.

TABLE IV. Sand slag discharge efficiency table.

MALMSTONE	20°	25°	30°	35°	40°
0	0. 06	0. 17	0. 51	65. 52	98. 42
2. 5	6. 11	20. 19	20. 76	47. 8	-
5	12. 56	39. 44	70. 08	77. 32	-
10	94. 02	97. 86	98. 36	98. 89	-

4.2 Analysis of experimental results of slag discharge efficiency.

According to the data, the slag discharge efficiency of each rock slag under different

Forest Chemicals Revew
www.forestchemicalsreview.com
ISSN: 1520-0191
July-August 2021 Page No. 974-988
Article History: Received: 12 May 2021 Revised: 25 June 2021 Accepted: 22 July 2021 Publication: 31 August 2021

conditions is obtained, as shown in Table IV. According to the data, the change chart of slag discharge rate of sandstone is generated, as shown in Fig 7.

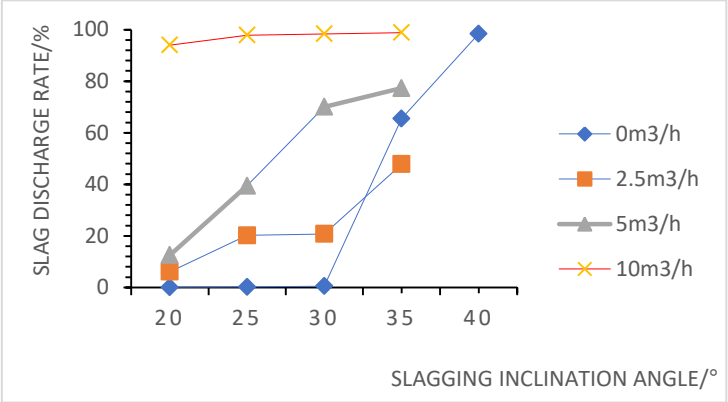

Fig 7: Variation diagram of slag discharge rate of sandstone.

It can be seen from Fig 7 that when the reaming angle of reverse well drilling is 20, the slag removal efficiency of sandstone is higher under the auxiliary condition of water flow and drainage of $10m^3/h$; When the reaming angle of reverse drilling is 25, the slag removal efficiency is higher with the aid of water flow of $10m^3/h$; When the reaming angle of reverse well drilling is 30, the slag removal efficiency is higher with the aid of water flow of $5m^3/h$ and $10m^3/h$; When the reaming angle of reverse well drilling is 35, the slag removal efficiency is higher with the aid of water flow of $5m^3/h$ and $10m^3/h$.

According to the analysis of the change curve of slag discharge effect of sandstone, the slag discharge can conform to the following rules: under the condition that other conditions are unchanged, the greater the inclination angle of reverse well, the better the slag discharge effect; The greater the auxiliary water discharge, the better the slag removal effect. When the inclination angle of reverse well reaming is greater than 30, the slag removal with $10m^3/h$ water flow can meet the slag removal requirements of sandstone slag.

4.3 Analysis of water-rock velocity test results.

The velocity measurement of slag-carrying water flow under the auxiliary condition of adding water in the test of reaming and deslagging in a small dip angle reverse well is mainly carried out by the image analysis method, which is the most widely used observation method in the debris flow velocity test, and the LS300A type flow velocimeter is used for auxiliary measurement in the observation dead zone of the image analysis method. The image analysis method is to record the whole process from the beginning of each group of slag discharge tests to the end of slag discharge by video camera and match and analyze the obtained video at every moment in the slag discharge process by professional software, to calculate the velocity of slag-carrying water flow in each period. The flow rate of sandstone slag is recorded according to the slag discharge angle and water discharge by image analysis method and

Forest Chemicals Revew
www.forestchemicalsreview.com
ISSN: 1520-0191
July-August 2021 Page No. 974-988
Article History: Received: 12 May 2021 Revised: 25 June 2021 Accepted: 22 July 2021 Publication: 31 August 2021

LS300A flow velocimeter, as shown in fig. 8-10 (l is the distance /m from the point on the runner to the top of the runner):

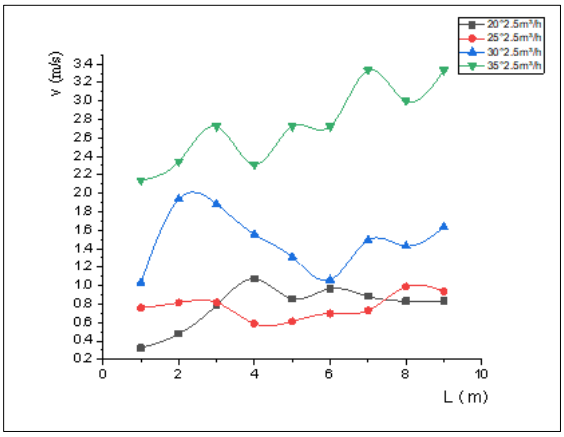

Fig 8: 2. 5m^3/h water slag velocity diagram.

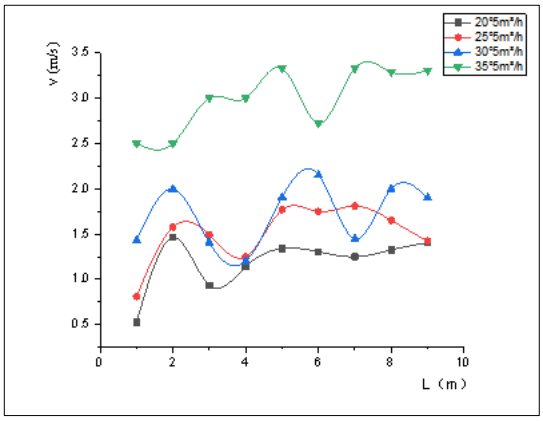

Fig 9: Flow velocity diagram of slag-carrying water of 5m^3/h.

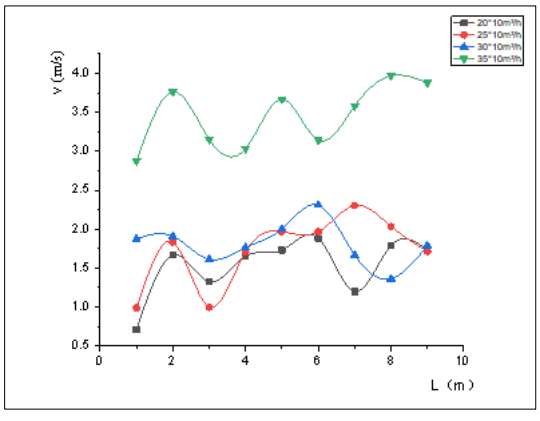

Fig 10: Flow velocity diagram of slag-carrying water of 10m^3/h.

It can be seen from fig. 8 to fig. 10 that under the condition of constant slag discharge angle, the greater the water discharge is, the greater the velocity of slag-carrying water flow is. From the velocity distribution of rock slag in the runner, the velocity of rock slag in the middle of the

Forest Chemicals Revew
www.forestchemicalsreview.com
ISSN: 1520-0191
July-August 2021 Page No. 974-988
Article History: Received: 12 May 2021 Revised: 25 June 2021 Accepted: 22 July 2021 Publication: 31 August 2021

runner tends to decrease, which is due to the agglomeration phenomenon of rock slag in the runner due to friction, which causes blockage in the runner and reduces the velocity of slag-carrying water flow. With the increase of the hydrodynamic pressure from above, the agglomerated rock slag is dispersed, and the velocity of slag-carrying water flow continues to increase.

4.4 Analysis of starting velocity of rock slag water flow.

Sandstone slag will be mixed with water flow in the process of slag removal by adding water, so the process of slag removal by sandstone can be compared with debris flow. According to the improved formula, the starting velocity of sand-laden water flow is used to evaluate the critical value of slag discharge, which is suitable for rock flow with large specific water and sand-laden water flow. The calculation method is:

$$V_c = \frac{m}{\sqrt{\gamma H\mu+1}} R^{\frac{2}{3}} I^{\frac{1}{10}} \quad (9)$$

Type is the velocity of slag-laden water flow, m/s; is the specific gravity of solid matter in slag-laden water flow, t/m^3. is the correction coefficient, $\mu = \frac{\gamma C-1}{\gamma C-\gamma H}$, where R is the bulk density of slag-laden water flow, t/m^3. is the hydraulic radius of slag-laden water flow. is water surface gradient. m is the external resistance coefficient. According to Liu Dezhao's external resistance coefficient table, comparing the chute with the river channel bed, it can be known that the river reach is straight, the riverbed is flat, the cross section is rectangular or parabolic boulders or loess riverbed, and when the average grain size is 0. 001~0. 08m, the value of M can be taken as 7. 5 under the condition that the longitudinal gradient of the chute is I > 0. 015m.

The continuous water flow increases the internal water pressure of the rock slag heap, reduces the effective stress, and makes it too late for the water infiltrated by the sandstone rock slag to flow out. In addition, due to the effect of continuous water addition, the sandstone rock slag heap, which can be regarded as a solid loose material, will start up and start to fall with the water flow. At this point, the formula for judging the start of the rock slag heap is:

$$K = \frac{(\sigma-\mu_\omega)\tan\varphi+AC}{T+G\sin\beta} \quad (10)$$

Where, is the contact area between loose material and trench bed, and in this test, it is taken as the contact area between rock slag heap and chute. As the chute is semi-circular, take. is the weight of the rock slag pile. is the thrust of water flow, which can be ignored because the initial velocity of water flow is eliminated. is the chute inclination and is the stability coefficient of the rock slag pile. Equation (10) can also be regarded as:

Forest Chemicals Revew
www.forestchemicalsreview.com
ISSN: 1520-0191
July-August 2021 Page No. 974-988
Article History: Received: 12 May 2021 Revised: 25 June 2021 Accepted: 22 July 2021 Publication: 31 August 2021

$$K = \frac{F+LBC}{R+T} \quad (11)$$

When =1, the rock slag pile is in the limit state. When > 1, the rock slag pile is in a stable state and will not fall; When < 1, the rock slag pile is in an unstable state and will fall along the chute. Substituting each parameter into formula (11), the values under different conditions are shown in Table Ⅴ.

TABLE V. K Value of Sand Slag Discharge under Different Displacement.

ANGLE	2. 5m^3/h	5m^3/h	10m^3/h	10m^3/h
20	1. 604	0. 858	0. 560	0. 459
25	1. 298	0. 695	0. 453	0. 372
30	1. 095	0. 587	0. 383	0. 314
35	0. 957	0. 512	0. 334	0. 274

Comparing the obtained value with the slag removal efficiency in the test, it is found that the slag starts to fall when the value is less than 1, and the slag can be fully discharged when the value is less than 0. 7. The theory is in good agreement with the experiment. Compare the test data with the theoretical value calculated by the formula (5), and see Table Ⅵ for the starting velocity of rock slag under different conditions obtained by theoretical calculation.

Table VI. Start-up velocity table of sandstone under different conditions (unit: m/s)

	20	25	30	35
2. 5	4. 798	2. 211	1. 971	1. 544
5	1. 712	1. 461	1. 268	0. 807
10	0. 662	0. 589	0. 399	0. 323

By comparing the water-rock flow velocity of sand rock slag in reverse hole reaming with small dip angle under different conditions with the starting velocity of the improved formula, it can be seen that when the actual velocity is greater than the starting velocity, the slag removal effect is more obvious. Because some of the slags in the test group with incomplete slag removal did not move along with the slag-carrying water flow during the test speed measurement, there are still some errors. To sum up, the start-up speed of rock slag from reaming and deslagging in reverse wells with a small dip angle can be calculated by using the improved formula.

V CONCLUSION

In this paper, the field test method is used to test the slag discharge of sandstone in small

Forest Chemicals Revew
www.forestchemicalsreview.com
ISSN: 1520-0191
July-August 2021 Page No. 974-988
Article History: Received: 12 May 2021 Revised: 25 June 2021 Accepted: 22 July 2021 Publication: 31 August 2021

angle reverse drilling and reaming. Through the research and analysis of the characteristics, efficiency and start-up velocity of sandstone slag discharge during the test, the main conclusions are as follows:

1) Through analyzing the slag removal movement of sandstone in reverse hole reaming at 20-35, and calculating its start-up speed by using the improved formula, it is concluded that the critical start-up speed of slag-laden water flow in reverse hole reaming at 20-35 is in the range of 0-5m/s under different displacements.

2) When the angle of slag discharge is 20 or above, the slag can be fully discharged with the aid of $10m^3$/h water flow, and when the angle of slag discharge is 30 or above, the slag can be fully discharged with the aid of $5m^3$/h water flow.

3) The factors affecting the slag discharge effect of reaming drilling with reverse drilling rig in inclined shaft with 20-35 inclination angle are slag discharge inclination angle, slag type and water discharge. Under the condition that other conditions are unchanged, the greater the angle of slag discharge, the better the slag discharge effect. The greater the water discharge, the better the slag removal effect.

4) When K<1, sandstone starts to have a downward slag discharge trend; When K<0. 7, sandstone has obvious slag removal effect. According to the k value, it can be concluded that when the hole angle in the reverse well is 20, the sandstone slag with the scouring water amount more than $10m^3$ has obvious slag removal effect. When the hole angle of the reverse well is 25, the sand rock slag with the scouring water amount larger than $5m^3$ has obvious slag removal effect. When the hole angle of the reverse well is 30, the sand rock slag with the scouring water amount larger than $5m^3$ has obvious slag removal effect. When the hole angle of the reverse well is 35, the sand rock slag with the scouring water amount larger than $5m^3$ has obvious slag removal effect.

ACKNOWLEDGEMENT

Thanks for the subject: Research on the key technology of small-angle raise drilling for rock mass mountain crossing, the subject number is:GK-2021-19. Thanks for the subject: Humanities and Social Science Research Project of Hebei Education Department (project ID: SQ2021058).

REFERENCES

[1]Shaterpour-Mamaghani, Copur, Hanifi. Empirical Performance Prediction for Raise Boring Machines Based on Rock Properties, Pilot Hole Drilling Data and Raise Inclination. Rock mechanics and rock engingering. 2021. 54(4):1707-1730

[2]Li Yingquan; Song Zhaoyang; Jing Guoye. The influence of the drilling rate of the raise boring

Forest Chemicals Revew
www.forestchemicalsreview.com
ISSN: 1520-0191
July-August 2021 Page No. 974-988
Article History: Received: 12 May 2021 Revised: 25 June 2021 Accepted: 22 July 2021 Publication: 31 August 2021

machine on the stability of the surrounding rock of a inclined shaft with large dip angle. 2020 International Symposium on Energy Environment and Green Development. 2020. 657:1755-1315

[3]Hao Tan; Qiang, Liu Zh Jie, Tan Ping Meng Yi. Drilling parameters optimization of pick-shaped TCT for raising boring construction of Feng Ning pumped storage power station. 4th International Conference on Advances in Energy Resources and Environment Engineering. 2018. 237:1755-1315

[4]Shaterpour-Mamaghani, Aydin; Copur, Hanifi; Dogan, Engin; Erdogan, Tayfun. Development of new empirical models for performance estimation of a raise boring machine. Tunnelling and underground space tehnology. 2018. 82:428-441

[5]Shaterpour-Mamaghani, A; Bilgin, N; Balci, C; Avunduk, E; Polat, C. Predicting Performance of Raise Boring Machines Using Empirical Models. Rock mechanics and rock engineering. AUG 2016. 49(8):3377-3385

[6]Liu, Zhiqiang; meng, Yiping. Key technologies of drilling process with raise boring method. Rock mechanics and rock engingering. 2015. 7(4):385-394

[7]Liu, Zhiqiang; Meng, Yiping; Jing, Hongguang; Cai, Meifeng. Application of raise-boring method in construction of under- ground water- sealing caverns. 4th International Conference on New Development in Rock Mechanics and Engineering. SEP 14-17, 2019. 203-209

[8]Ashrafi, Seyed Babak; Anemangely, Mohammad; Sabah, Mohammad; et al. Application of hybrid artificial neural networks for predicting rate of penetration (ROP): A case study from Marun oil field. Journal of Petroleum Science and Engineering. 2019. 175:604-623

[9]Behboud, M. Mohammadi; Ramezanzadeh, A. ; Tokhmechi, B. i. Studying empirical correlation between drilling specific energy and geo-mechanical parameters in an oil field in SW Iran. journal of mining and environment. 2017. 8(3):393-401

[10]Calder, P. N. Rock Mechanics aspects of large hole boring machine design. Journal of mining and environment. 2019. 11:159-175

[11]Copur, H; Bilgin, N; Tuncdemir, H; et al. A set of indices based on indentation tests for assessment of rock cutting performance and rock properties. journal of the southern african institute of mining and metallurgy. 2020. 103(9):589-599

[12]Copur, Hanifi; Bilgin, Nuh; Balci, Cemal; et al. Effects of Different Cutting Patterns and Experimental Conditions on the Performance of a Conical Drag Tool. Rock mechanics and rock engingering. 2017. 50(6):1585-1609

[13]Dollinger, GL; Handewith, HJ; Breeds, CD. Use of the punch test for estimating TBM performance. Tunnelling and underground space technology. 2021. 13(4):403-408

[14]Dougherty, Patrick S. M.; Pudjoprawoto, Randyka; Higgs, C. Fred, III. Bit cutter-on-rock tribometry: Analyzing friction and rate-of-penetration for deep well drilling substrates. Triboligy international. 2019. 77:178-185

[15]Anonymous. Market scale and future development prospects of the energy storage power station industry in 2019. Rock mechanics and rock engineering. 2019. 12:44-50